Title page

Seasonal controls on the diet, metabolic activity, tissue reserves and growth of the cold-water coral *Lophelia pertusa*

Sandra R. Maier[1], Raymond J. Bannister[2], Dick van Oevelen[1]*, and Tina Kutti[2]*

* *shared last authors*

1: Department of Estuarine and Delta Systems, Royal Netherlands Institute for Sea Research (NIOZ-Yerseke) and Utrecht University, Yerseke, The Netherlands

2: IMR Institute of Marine Research, Nordnesgaten 50, 5005 Bergen, Norway

Corresponding authors

Dick van Oevelen,[1], dick.van.oevelen@nioz.nl

Sandra R. Maier,[1], sandra.maier@nioz.nl

Key words:

Deep sea, food supply, fatty acid, amino acid, stable isotopes, compound-specific

Abstract

Vast cold-water coral (CWC) reefs occur in temperate regions, where strong seasonality in temperature and light leads to a short but highly productive spring period. How CWCs respond physiologically to this strong seasonal forcing remains unclear, due to the remoteness of their deep-sea habitats. In an *in situ* transplantation study at Nakken reef, Norway, we investigated a full seasonal cycle of (1) temperature and food availability, (2) diet, (3) biomass and tissue reserves, (4) oxygen consumption, and (5) linear growth of the reef-building coral *Lophelia pertusa*. All investigated variables showed a distinct seasonality. An increase in the organic carbon and amino acid content, linear extension and budding rate from February to late May, at a simultaneous increase of phytoplankton- and zooplankton-fatty acid trophic markers (FATMs), and $\delta^{15}N$-derived trophic level, indicates an efficient exploitation of the spring phytoplankton- and the subsequent zooplankton bloom. A pool of neutral-lipid-derived fatty acids (NLFAs), indicative of energy storage and gametogenesis, was formed from May to October, accompanied by increased oxygen consumption, i.e., metabolic activity. In late autumn and early winter (October to December), tissue reserves were maintained, in spite of low sPOM and zooplankton food availability, and the lower tissue $\delta^{13}C$ and higher contribution of bacterial FATMs suggest increased reliance on more degraded material. The concurrent reduction in linear growth further suggests a lower energy availability at this time of the year. A large (>50%) drop of all tissue pools between December and February coincided with the spawning season of *L. pertusa*, and demonstrates a high energetic cost of reproduction. Our results show for the first time a strong seasonal control of critical life history traits such as growth patterns and timing of reproduction in this prominent deep-sea species.

Introduction

Diverse and productive cold-water coral (CWC) reefs are frequently found at high latitudes that are characterised by a pronounced seasonality, including the North East Atlantic Ocean (Freiwald 2002; Roberts et al. 2006). The dominant reef-forming species here is *Lophelia pertusa* (syn. *Desmophyllum pertusum*, Addamo et al. 2016), which feeds on surface-derived organic matter and zooplankton (Duineveld et al. 2004; Kiriakoulakis et al. 2005; van Oevelen et al. 2018). The transport of this surface material to the deep reefs is facilitated by hydrodynamic mechanisms (Frederiksen et al. 1992; Thiem et al. 2006), and zooplankton migrations (Jónasdóttir et al. 2015; Van Engeland et al. 2019). However, in high latitude waters, the phytoplankton production and export to the deep-sea undergoes a typical seasonal succession, from very low values in winter to spring bloom conditions (Duineveld et al. 2004, 2007; Lavaleye et al. 2009).

Seasonally varying food availability requires (1) a high resource flexibility, (2) efficient tissue storage, and/or (3) an adaptation of growth and metabolic rate. Feeding experiments have shown that *L. pertusa* is able to consume DOM and bacteria (Mueller et al. 2014), and to even convene chemoautotrophic pathways (Middelburg et al. 2015). Furthermore, *L. pertusa* contains large amounts of storage lipids (triacylglycerides and wax esters, Dodds et al. 2009), which they build-up during experimental food pulses, and deplete during subsequent food deprivation (Maier et al. 2019). However, experimental food deprivation causes a relatively low reduction of metabolic rates, and no reduction of skeletal growth (Larsson et al. 2013; Maier et al. 2019).

The growing body of experimental studies on CWC adaptation to variable food availability is in stark contrast to the limited *in situ* data, owing to the low accessibility of their remote deep-sea habitats, especially in autumn and winter. To date, one study has addressed the seasonal development of CWC lipid stocks, and found no significant change of lipid content

or composition over the year (Dodds et al. 2009). *In situ* time series on seasonal CWC performance are, however, crucial, since global climate change might alter the seasonal forcing, and hence the phenology, i.e., seasonal activity of organisms (Walther et al. 2002).

We present an integrative full-year dataset from an *in situ* transplantation experiment, in which corals (*L. pertusa*) were repeatedly transplanted to a reef in a Norwegian fjord, and recollected. We evaluate the seasonal controls of varying temperature and food availability, i.e., suspended particulate organic matter (sPOM, above-reef) and zooplankton (entire water column), on their diet (1), tissue reserves (2), metabolic activity (oxygen consumption) (3), and linear skeletal growth (4). Diet shifts were inferred from a combination of trophic markers, including tissue $\delta^{13}C$ and $\delta^{15}N$ (Fry 2006; Michener and Lajtha 2008), amino-acid-specific $\delta^{15}N$ (McClelland and Montoya 2002; Chikaraishi et al. 2009), and fatty acid trophic markers (FATMs; Dalsgaard et al. 2003; Kelly and Scheibling 2012).

Materials and methods

Site description

The Nakken reef (59°49.89N, 05°33.38E) is located 30-40 km south of Bergen, western Norway, at the intersection of Hardanger and Langenuen fjord (Figure 1a). Patchily distributed live coral colonies (height: 1-2 m, diameter: up to 4 m) grow on a base of dead coral framework (Figure 1b), particularly densely in a slightly elevated 200 x 200 m^2 area at 220-200 m depth (Figure 1c).

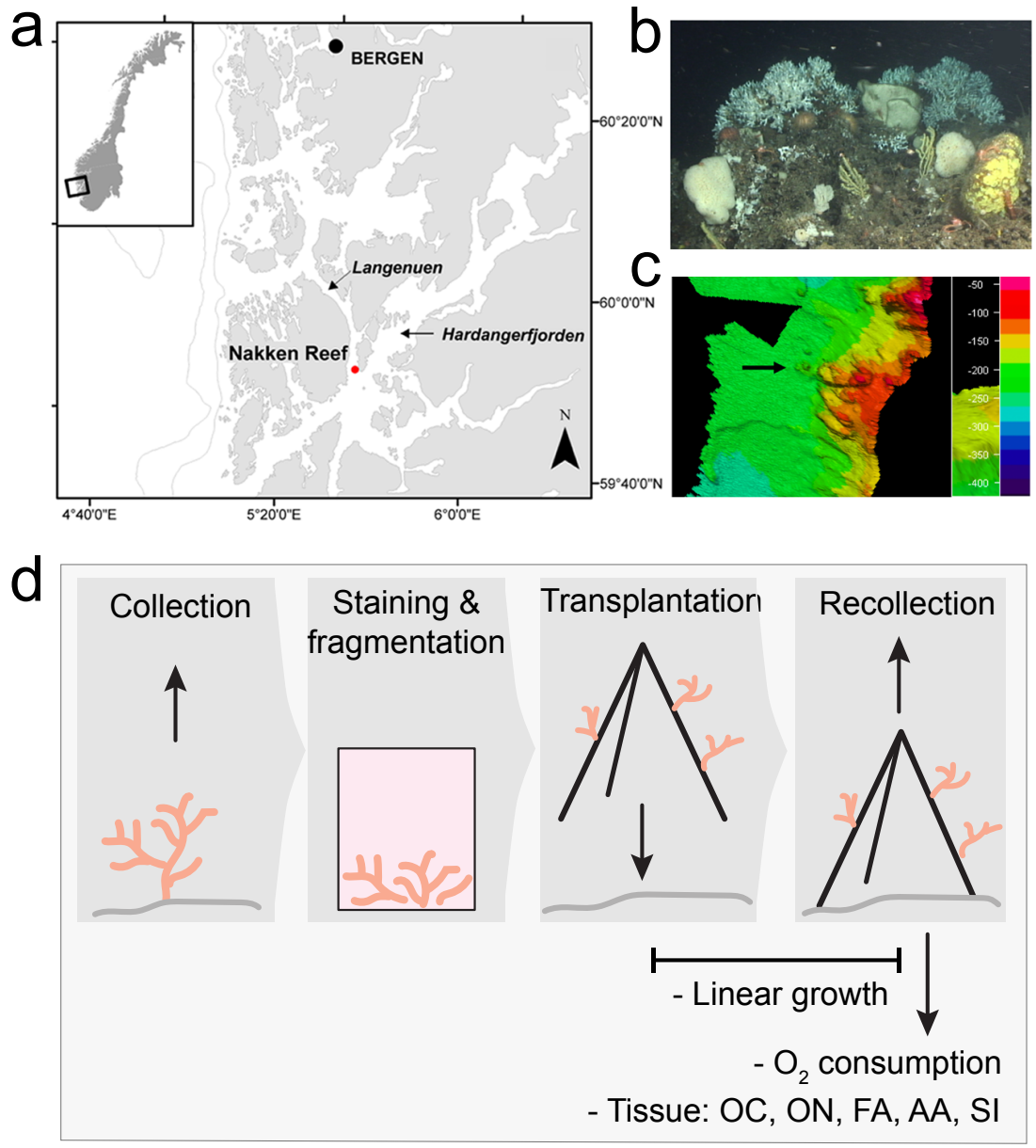

Figure 1: Study site and transplantation experiment. (a) Location of Nakken reef at the intersection of Hardanger and Langenuen fjord, western Norway. (b) Live coral colonies (*Lophelia pertusa*) grow in patches on a base of dead coral framework, particularly densely in an area of elevated seafloor (c, indicated by arrow). (d) Workflow of transplantation experiment (OC: organic carbon, ON: organic nitrogen, FA: fatty acids, AA: amino acids, SI: stable isotopes).

Transplantation experiment

The *in situ* transplantation experiment (Figure 1d, Table 1) consisted of several seasonal rounds of (1) *L. pertusa* collection from Nakken reef, (2) coral staining for skeletal growth measurement, (3) transplantation back to the reef, and (4) recollection several months later to

99 assess skeletal linear extension ('Linear growth'), oxygen consumption as a measure of
100 metabolic activity, tissue reserves and trophic markers ('Tissue samples'). The time points of
101 recollection will be referred to as 'season' (Table 1). An additional set of corals was collected
102 at the end of May 2014, and (without transplantation) used to measure oxygen consumption,
103 tissue reserves and trophic markers.
104 Coral samples were collected using the ROV *Aglantha* (run by the Institute of Marine
105 Research, IMR), brought to the surface in a closed ROV-biobox, and transferred without air
106 exposure to a tank with deep water, collected on-site from 100 m depth. Exposure to sunlight
107 was kept to a minimum (2-15 min). Corals were transported to Austevoll Research Station
108 (IMR, 1.5 h sailing time), where they were maintained in the dark in 1,000 L flow-through
109 tanks receiving unfiltered deep water from Langenuen fjord (160 m depth) at a rate of 200 L
110 h^{-1} until transplantation.
111 The coral skeleton was stained with 10 mg L^{-1} Alizarin red in 200 L-aerated tanks for 48 h
112 (Brooke and Young 2009). Fragments were clipped from the stained coral samples (for
113 replication see Table 1), and placed in a non-toxic epoxy putty in transplant units made of 2
114 cm PVC pipes filled with cement. The transplant units were left to harden in an aerated sea-
115 water tank and then placed back in the flow-through tanks.
116 The coral transplant units were transported back from Austevoll to the Nakken reef site in
117 deep-water-filled cooling containers (1.5-3 h). Before deployment, they were fastened with
118 cable ties to three modified scallop cultivation trays, which were attached to moorings, and
119 deployed 5 m above the sea-bed in the centre of Nakken reef. They were recovered after 2.5
120 to 4.7 months (Table 1). Air exposure during deployment and recollection was kept to a
121 minimum (1 min). After recollection, the transplanted coral fragments (or subsets, see Table
122 1) were incubated on-board to measure oxygen consumption, then measured for linear
123 growth, and thereafter frozen (-20 °C) for later tissue analysis. The oxygen consumption of

the non-transplanted corals was measured on-board after collection (May 2014), before they were frozen.

Table 1: Coral transplantation experiment, metadata: dates, cruises, replicates (n). For explanation of experiment, see Figure 1d. Colour code (filling/text colour) to connect measured parameters with measurement dates/periods.

Season (month)	Collection		Transplantation		Recollection	Transplantation duration [months]	Linear growth		O_2 con-sump-tion	Tissue samples
	Date	Cruise	Date	n	Date		Period	n	n	n
Dec_13	Sep 2013	RV H. Mosby # 2013621	29 Sep 2013	7	13 Dec 2013	2.5	Oct-Dec	7	5	12
Mar_14			29 Sep 2013	5	27 Mar 2014	3.5	Dec-Mar (Dec-Mar min. Oct-Dec)	5	5	5
May/ Jun_14	May 2014	RV H. Mosby # 2014611	NA		NA		NA		5	6
Oct_14			02 Jun 2014	5	22 Oct 2014	4.7	Jun-Oct	5	5	5
Feb_15	Jul 2014	RV G.O. Sars # 2014111	28 Oct 2014	5	09 Feb 2015	3.5	Oct-Feb	5	NA	5

Oxygen consumption

Directly after (re-)collection, corals were transferred to 1 L- cylindrical, acrylic incubation chambers, partly submerged in a cooled (8 °C) water bath, and supplied with a flow-through (20 mL min^{-1}) of unfiltered deep water collected on-site with Niskin bottles. After coral recovery, indicated by fully-extended polyps (1-2 h), chambers were closed air-tight, and incubated for 7-12 h. A stirrer in the lid created a circular flow to ensure mixing. The oxygen concentration was continuously logged with PreSens micro-optodes inserted through the chamber lid. One seawater-only control was carried out per incubation run to control for potential O_2 consumption by plankton. The coral O_2 fluxes were calculated by linear

140 regression, corrected for O_2 fluxes in the seawater controls, and standardized to coral dry
141 mass.
142
143 **Linear growth and polyp budding**
144 From each of the transplanted coral fragments, we measured the linear extension of 5-7
145 terminal polyps from their alizarin stained band to the outer edge of their calices, according
146 to Brooke and Young (2009). Polyps were therefore externally photographed using a Leica
147 (MZ7) stereo microscope connected to a Q IMAGING RoTS camera. Linear extension was
148 measured on these pictures, using QCapture and Image J photo software, and expressed as
149 mm $polyp^{-1}$ $month^{-1}$. Polyps were categorized in (a) old terminal polyps, i.e., polyps that were
150 stained before transplantation, (b) young terminal polyps, i.e., polyps that were growing on
151 old terminal polyps and were likewise stained before transplantation, and (c) new polyps, i.e.,
152 non-stained polyps that formed during the transplantation period. The linear growth of old,
153 young and new polyps of coral fragments transplanted in October 2013 and recollected in
154 March 2014 ('Oct13-Mar14') was corrected for the average linear polyp growth from
155 'Oct13-Dec13', to calculate linear growth rates for the interval 'Dec13-Mar14' (Table 1).
156 The number of new polyps was additionally counted for each transplantation period to
157 elucidate when new polyps were formed (budding).
158
159 **Tissue analysis**
160 Coral samples were analysed for the following tissue parameters: organic carbon (OC),
161 organic nitrogen (ON), organic $\delta^{13}C$, organic $\delta^{15}N$, hydrolysable amino acid (AA)
162 concentration and AA-$\delta^{15}N$, neutral- and phospholipid-derived fatty acid (NLFA and PLFA)
163 concentration and NLFA- and PLFA-$\delta^{13}C$. Coral fragments were lyophilized, weighed (dry
164 mass, i.e., DM), and homogenized to fine coral powder with a ball mill. Extraction and

analytical procedures are described in detail in Maier et al. (2019). In brief, the OC content (in mmol OC gDM^{-1}) and $\delta^{13}C$ were analysed on decalcified samples on an elemental analyser coupled to an isotope ratio mass spectrometer (EA-IRMS), the ON content and $\delta^{15}N$ on non-decalcified samples on the same machine. Hydrolysable AAs were extracted according to Veuger et al. (2005) and Maier et al. (2019), by acidic hydrolyzation and derivatization with acidified isopropanol and pentafluoropropionic anhydride. Total lipids were extracted with a modified Bligh-Dyer extraction, according to Boschker et al. (1999) and Maier et al. (2019), separated based on polarity into neutral-lipid-derived fatty acids (NLFAs) and phospholipid-derived fatty acids (PLFAs) by silicic acid column chromatography, and derivatized by mild alkaline methanolysis. Concentrations of individual AAs, NLFAs and PLFAs (in e.g., mmol AA-C gDM^{-1}), and the AA-$\delta^{15}N$, NLFA- and PLFA-$\delta^{13}C$ were measured on a gas chromatograph (GC) ZB-5 MS column (Phenomenex, USA), coupled to an isotope ratio mass spectrometer (IRMS) via a THERMO combustion GC-c-III interface. The AA, NLFA and PLFA concentrations were corrected for C-atoms added during derivatization, the AA concentration additionally for the AA recovery efficiency (Maier et al. 2019).

Temperature and food availability

The temperature at Nakken reef (6 m above bottom) from December 2013 to October 2014 was extracted from the NorKyst-800 numerical ocean modelling system (Albretsen 2011). sPOM samples were taken with Niskin bottles 3-5 m above the reef during most seasons (Table 2). 3-10 L of water was filtered over pre-combusted, pre-weighed 47 mm GF/F filters to retain material >0.7 μm. Filters were dried to constant weight at 60 ºC (sPOM-dry mass). A filter subsample (5%) was analysed on the EA-IRMS for OC, ON, $\delta^{13}C$, and $\delta^{15}N$. For every season, some entire filters were used for AA-and NLFA/PLFA- instead of CN-analysis

(Table 2). Their sPOC and sPON concentration was estimated from their dry mass, and the %OC measured on other filters of the same season. AAs were extracted from the sPOM samples (Table 2) according to Grosse et al. (2015), NLFAs and PLFAs as described for the coral tissue. Concentration, $\delta^{13}C$ and $\delta^{15}N$ of AAs, and concentration and $\delta^{13}C$ of NLFAs and PLFAs was measured as described above.

Zooplankton was sampled with a 180-µm-WP2 net (diameter: 0.57 m), in vertical hauls from 10 m above the reef (190 m depth) to the surface or from 100 m depth to the surface, at the time points indicated in Table 2. Unlike sPOM concentrations, the zooplankton concentrations are integrated over the water column above the reef rather than on-reef concentrations, but zooplankton from shallower depth is assumed to migrate from shallower depths to the reef on a daily basis (Jónasdóttir et al. 2015; Van Engeland et al. 2019). Zooplankton samples were processed and analysed for zooplankton-C-and -N concentration (µmol C or N (L of filtered water)$^{-1}$), AAs, NLFAs and PLFAs and the respective $\delta^{13}C$ and $\delta^{15}N$ as described for the coral tissue.

Table 2: Sampling and analysis of zooplankton and suspended particulate organic matter, metadata: dates, and analysed replicates (n) for CN (carbon, nitrogen), FA (fatty acids) and AA (amino acids). For cruises see table 1.

Season (month)	Zooplankton					sPOM				
	Date	Depth [m]	CN [n]	FA [n]	AA [n]	Date	Depth [m]	CN [n]	FA [n]	AA [n]
Dec_13	11 Dec 2013	190 to 0	3	3	3	12 Dec 2013	190	3	1	2
Mar_14	NA					27 Mar 2014	190	1	1	1
May/ Jun_14	27 May 2014	190 to 0	4	4	1	26 May 2014	190	1	1	1
Oct_14	NA					NA				
Feb_15	09 Feb 2015	100 to 0	3	1	1	09 Feb 2015	190	1	1	1

209 **Data analysis**

210 Graphical and statistical analysis was done with R (R Core Team 2017). Statistical
211 significance is based on a probability value $p < 0.05$. P values are given in text, detailed
212 results of statistical analyses are provided as online resources (S1, S2).

213

214 *Seasonality of coral physiology and food availability*

215 Non-parametric Kruskal-Wallis rank sum tests ('Kruskal') with post-hoc Dunn tests ('Dunn',
216 R-package FSA, Ogle et al. 2018) were applied for seasonal comparison of coral OC and ON
217 content (biomass), summed AA concentration, summed NFLA and PLFA concentration,
218 oxygen consumption and linear growth rate (in mm polyp^{-1} month^{-1}, independent of polyp
219 categories old, young, new; because nesting 'polyp categories' in 'season' is not possible in
220 the required non-parametric test). The same statistics was applied to detect seasonal
221 differences in food availability (concentration of sPOC, zooplankton-C). Linear models (lm)
222 served to test the influence of temperature on dry-mass-specific coral oxygen consumption
223 (lm1), the influence of coral OC (seasonal average, lm2) and the combined influence of
224 temperature and coral OC (lm3).

225

226 *Trophic markers as indicators of seasonal diet shift*

227 Differences in $\delta^{13}C$ and $\delta^{15}N$ were analysed in stable isotope biplots (1) between corals,
228 sPOM and zooplankton, and (2) between corals of the different seasons. Differences in $\delta^{13}C$
229 and $\delta^{15}N$ were statistically assessed in separate Kruskal-Wallis and Dunn tests. Since fatty
230 acids (FAs) are depleted in $\delta^{13}C$, a varying FA content might confound the use of $\delta^{13}C$ as
231 trophic marker (Post et al. 2007). The $\delta^{13}C$ values of corals, sPOM and zooplankton are
232 therefore presented both as measured, and corrected for FA-$\delta^{13}C$ as $\delta^{13}C_{corr} =$
233 $\frac{\delta^{13}C_{tissue} \cdot c_{tissue-C} - \delta^{13}C_{FA} \cdot c_{FA-C}}{c_{tissue-C} - c_{FA-C}}$, where $c_{FA\text{-}C}$ is the summed NLFA- or PLFA-C

concentration, $c_{tissue\text{-}C}$ the coral OC content, and $\delta^{13}C_{FA}$ the NLFA/PLFA-$\delta^{13}C$ derived as weighted average from the $\delta^{13}C$ of the individual NLFAs/PLFAs. Seasonal increases in coral-$\delta^{13}C$ were interpreted as consumption of a higher trophic level (Fry, 2006), and/or consumption of fresher material, based on the high $\delta^{13}C$ of chlorophyll-a-derived C (Miller et al. 2008).

The trophic level of corals was assessed for every season, (a) based on their bulk tissue $\delta^{15}N$ ('tissue-$\delta^{15}N$-derived trophic level'), compared with the sPOM-$\delta^{15}N$ and zooplankton-$\delta^{15}N$, assuming a trophic fractionation factor of 2.2‰ to 3.4‰ (Fry, 2006); (b) as 'AA-$\delta^{15}N$-derived trophic level', based on the $\delta^{15}N$ of the 'trophic' AA phenylalanine, which becomes enriched with every trophic level (McClelland and Montoya 2002), and the non-enriched 'source' AA glutamine/glutamic-acid, as $TL_{Glu-Phe} = \frac{\delta^{15}N_{Glu} - \delta^{15}N_{Phe} - 3.4}{7.6} + 1$, according to Chikaraishi et al. (2009).

Seasonal patterns in fatty acid trophic markers (FATM, table 3), i.e., the percentage of zooplankton-, phytoplankton-, or bacteria-specific FAs in coral tissue, were analysed by Kruskal-Wallis and Dunn tests (Dalsgaard et al. 2003; Kelly and Scheibling 2012).

The similarity of AA, NLFA and PLFA composition between corals, sPOM and zooplankton (fixed factor 1: 'type') and between the seasons (fixed factor 2: 'season') was analysed with a 2-factor permutational ANOVA ('Permanova 1'), based on a Bray-Curtis similarity matrix on non-transformed data (R package vegan, Oksanen et al. 2018). Further, the respective compound compositions were compared between corals-only of the different seasons in a 1-factor ('season') Permanova ('Permanova 2'). For significant season-effects, additional pairwise comparisons between the seasons were carried out here, with the R-function pairwise.adonis (Martinez 2019), and 'Bonferroni'-adjusted p-values. Biplots of non-parametrical multidimensional scaling (nmds) of non-transformed data were used to illustrate the respective compositional similarities, analogous to Permanova 1 and 2. Finally, the AAs,

NLFAs or PLFAs causing the seasonal coral differences observed in Permanova 2 were identified in a SIMPER (SIMilarities PERcentages) analysis.

Results

Seasonality of the environment

Modelled temperatures at Nakken reef from December 2013 to February 2015 ranged from 6.5 °C to 9.2 °C. Temperatures were higher in autumn and winter, i.e., from mid-September to end of March, and lower over spring and summer, i.e., from beginning of April to September (Figure 2).

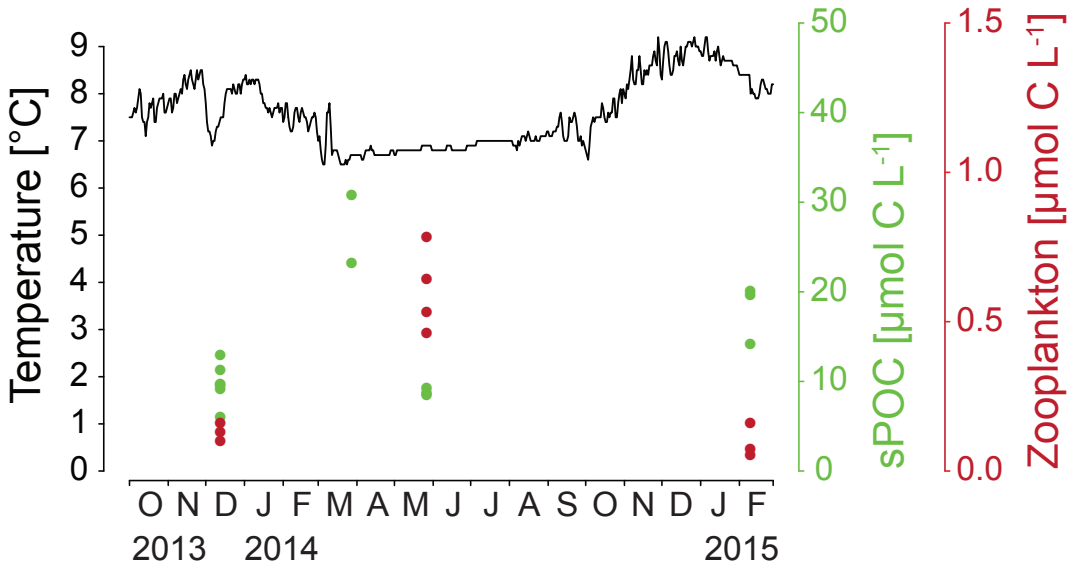

Figure 2: Seasonality of the environment at Nakken reef: Modelled temperature (in black) 6 m above bottom, and food availability, i.e., concentration of suspended particulate organic carbon (sPOC, in green) 3-5 m above the reef, and zooplankton-C-concentration (in red) in the water column above the reef. Letters: months from October 2013 to February 2015.

The concentration of suspended particulate organic carbon and nitrogen (sPOC, sPON) above the reef (Figure 2) increased from December 2013 to March 2014, and had decreased again to low winter-levels by late May 2014. The sPOC and sPON concentration was higher in February 2015, compared to December 2013. The zooplankton-C concentration in the water

column followed the sPOC concentration with a time lag of ± 2 months (Figure 2), and was low in December and February, and high at the end of May.

Tissue reserves

The OC content of *L. pertusa* differed significantly between seasons (Figure 3a, b; Kruskal, $p = 0.0$; Online Resource S1-1), with highest values in December 2013, and lowest values in February 2015, indicating a drop in OC between December and February. The OC steadily increased in spring, i.e., from March 2014 to late May 2014, following the development of the sPOC and zooplankton-C concentration. The ON content showed a similar trend. The CN ratio of corals was higher in October and December than in February, March and May (Online Resource S3). About 65% of the coral OC was accounted for by the analysed tissue pools (AAs, NLFAs and PLFAs), which showed a similar seasonal trend as the OC content, with highest concentrations in December, and significantly lower concentrations in February (Figure 3c, Kruskal, Dunn, $p < 0.05$). Like the OC content, the AA concentration increased already from February to May, while the NLFA concentration increased later, from May to October.

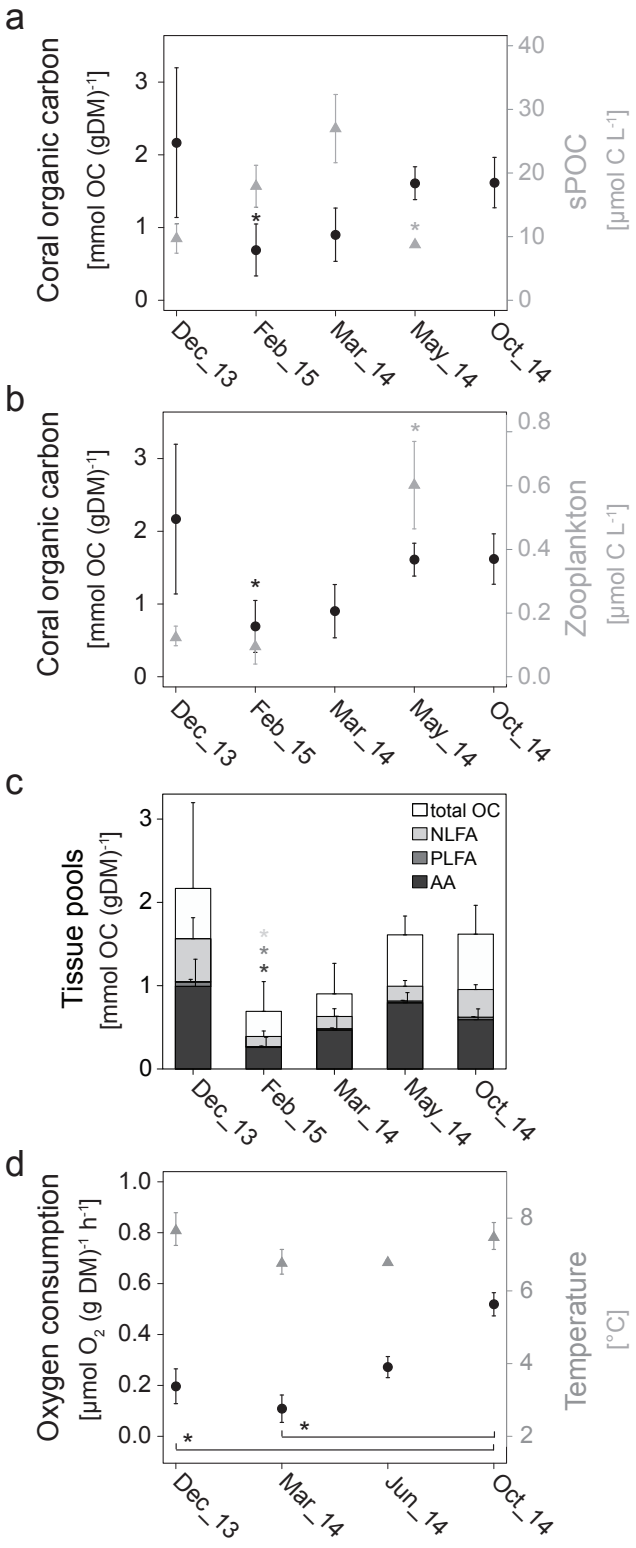

Figure 3: Seasonal environmental controls on tissue reserves and metabolic activity of *Lophelia pertusa*. (a, b) seasonal control of food availability (concentration of suspended particulate organic carbon, i.e., sPOC, and zooplankton; in grey) on coral organic carbon (OC) content (in black); (c) tissue pools amino acids (AA), neutral-and phospholipid-derived fatty acids (NLFA, PLFA) in relation to total coral OC; (d) oxygen consumption (in black) in relation to modelled temperature (in grey). All coral parameters are normalized to coral dry mass (DM). For clearer illustration of seasonal development, the time axis is non-continuous. *: data point(s) significantly different ($p < 0.05$) from previous data point(s)/data point indicated by bracket.

303

304 **Oxygen consumption**

305 The oxygen consumption of *L. pertusa* (Figure 3d) was lower in December and March, and
306 increased significantly from March to October (Kruskal, Dunn p = 0.0, Online Resource S1-
307 2). The O_2 consumption peak in October coincided with a high monthly average model
308 temperature (7.5 °C), but in December 2013, O_2 consumption rates were low in spite of high
309 temperatures (7.7 °C). Variability in temperature and coral OC content alone did not explain
310 the variability in coral O_2 consumption (linear models lm1, lm2, $p > 0.05$, Online Resource
311 S1-4), but the combination 'temperature x OC' content explained 89% of the variability in O_2
312 consumption, and the linear relation was significant (lm3, $p < 0.05$).

313

314 **Linear growth and polyp budding**

315 *Lophelia pertusa* terminal polyps showed skeletal linear growth throughout the year, with
316 rates varying significantly with season (Figure 4, Kruskal, p = 0.0). Linear growth rate per
317 polyp (independent of polyp type young, old or new) was significantly lower from October to
318 December than from December to March (Dunn, p = 0, Online Resource S1-2), and from
319 June to October (Dunn, p = 0). Linear growth rate decreased with polyp age, with new polyps
320 growing fastest (1.1 ± 0.2 mm polyp^{-1} month^{-1}), and old polyps slowest (0.3 ± 0.3 mm polyp^{-1}
321 month^{-1}). New polyps were formed from December 2013 to March 2014 and from October
322 2014 to February 2015, i.e., polyp budding occurred most likely between December and
323 February/March.

324

325

326

327

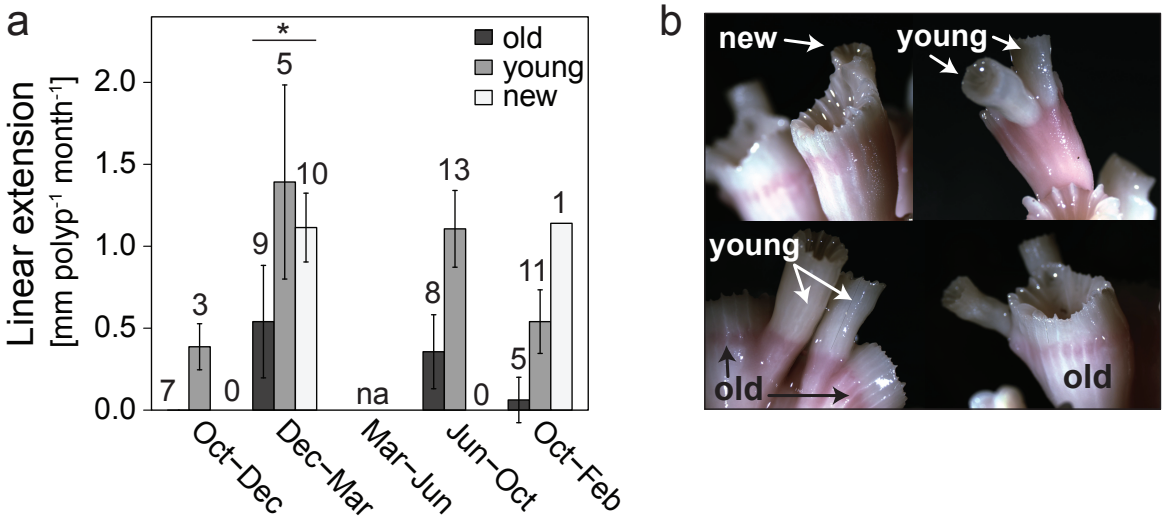

Figure 4: (a) Linear extension of *Lophelia pertusa* old, young, and newly formed terminal polyps over the indicated time periods. Numbers above bars indicate the numbers of examined polyps. *: linear extension (mean of old, young, new) in this period significantly different from previous period. (b) Old, young and new terminal polyps.

Isotope composition of coral tissue and amino acids

The $\delta^{13}C$ of *L. pertusa* (-24.2‰ to -21.9‰) was comparable to the $\delta^{13}C$ of zooplankton (-23.7‰ to -22.6‰), and significantly higher than the $\delta^{13}C$ of sPOM (-27.8‰ to -24.8‰, Figure 5a, Dunn, p = 0.0, Online Resource S1-2). The high variability in sPOM-$\delta^{13}C$ was mostly caused by low values in February (-27.8‰). The $\delta^{13}C$ of *L. pertusa* differed significantly between the seasons (Kruskal, p = 0), with a lower $\delta^{13}C$ in October and December, and a higher $\delta^{13}C$ in March and late May (Figure 5a). Significant differences between the seasons remained after the fatty-acid correction of $\delta^{13}C$-values (Figure 5b, Kruskal, p = 0).

The $\delta^{15}N$ (8.5‰ to 11.5‰) of the corals was significantly higher than the $\delta^{15}N$ of zooplankton (7.5‰ to 9.5‰) and sPOM (3.4‰ to 8.4‰, Kruskal, Dunn, p = 0). The high variability in sPOM-$\delta^{15}N$ was mostly caused by two samples with very low values in December (Figure 5a). The mean difference in $\delta^{15}N$ between corals and zooplankton (2.2‰) spans one trophic level or less, while the difference in $\delta^{15}N$ between corals and sPOM (3.7‰)

spans more than one trophic level. The coral tissue showed significant seasonal differences in tissue-$\delta^{15}N$ (Kruskal, $p = 0$), with highest values in late May (Figure 5a, Dunn not significant, $p > 0.05$).

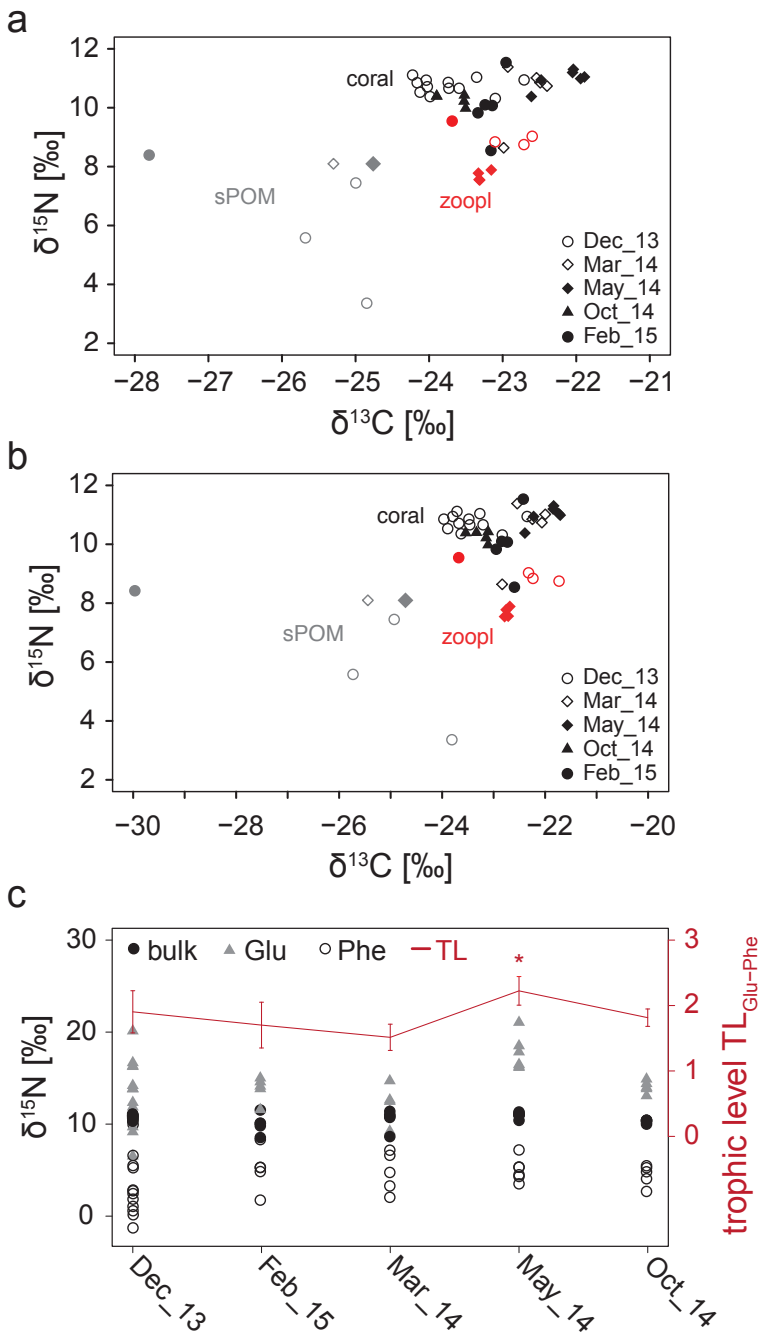

Figure 5: Isotope $\delta^{13}C$ and $\delta^{15}N$ composition of *Lophelia pertusa,* zooplankton and suspended particulate organic matter (sPOM). (a) $\delta^{13}C\delta^{15}N$ composition of corals (black) in comparison with zooplankton (red) and sPOM (grey) over the seasons (legend). (b) like (a), but with fatty-acid corrected $\delta^{13}C$ values. (c) $\delta^{15}N$ of coral tissue and the amino acids glutamic acid/glutamine and phenylalanine over the seasons; in red: trophic level calculated from $\delta^{15}N_{Glu}$ and $\delta^{15}N_{Phe}$ based on Chikaraichi et al., 2009. *: data point significantly different ($p < 0.05$) from previous data point.

358 The trophic level estimates based on the AA-δ^{15}N-analysis of phenylalanine (source AA,
359 stable throughout the months, Figure 5c) and glutamine/glutamic acid (trophic AA, more
360 variable) indicate a similar, annually-averaged trophic level for corals (1.9 ± 0.3) and
361 zooplankton (2.2 ± 0.2). The glutamine/glutamic acid-δ^{15}N and hence trophic level estimate
362 of *L. pertusa* was highest in May (2.2 ± 0.2). Trophic level estimates based on δ^{15}N-analysis
363 of other AA-pairs (i.e., phenylalanine versus proline, isoleucine, valine and alanine) were
364 slightly higher (2.3 ± 1, Online Resource S3), but do not support an increase in trophic level
365 in May.
366
367 **Fatty acid and amino acid composition**
368 The coral AA, NLFA and PLFA composition (Figure 6) differed significantly from
369 zooplankton and sPOM (Permanova 1, p_{NLFA}, p_{PLFA}, p_{AA} = 0.01, Online Resource S2-3a). In
370 terms of their NLFA and PLFA composition, corals and zooplankton were more similar to
371 each other than to sPOM, which showed a high within-group variability (Figure 6, low
372 sample number of sPOM should be noted).
373 The NLFA, PLFA and AA composition of *L. pertusa* further showed significant differences
374 between the months (Permanova 2, p_{NLFA}, p_{PLFA}, p_{AA} = 0.01, Online Resource S2-3b).
375 Specifically in the NLFAs and PLFAs, December samples were most distinct from the other
376 months (pairwise comparison, Online Resource S2-3b). Results of the SIMPER analysis
377 (Online Resource S2-4) indicate that NLFA- and PLFA- differences of the December-
378 samples were mostly caused by a lower concentration of C22:1ω11 and C20:3ω3/C20:1ω9c
379 (Figure 6b, compounds '16', 6d compounds '15'), and a higher concentration of two
380 unknown fatty acids eluting at ecl19.4/20.5 (most likely another C20-polyunsaturated FA)
381 and ecl21.2 (most likely another C22-poly- or monounsaturated FA; Figure 6b, compounds

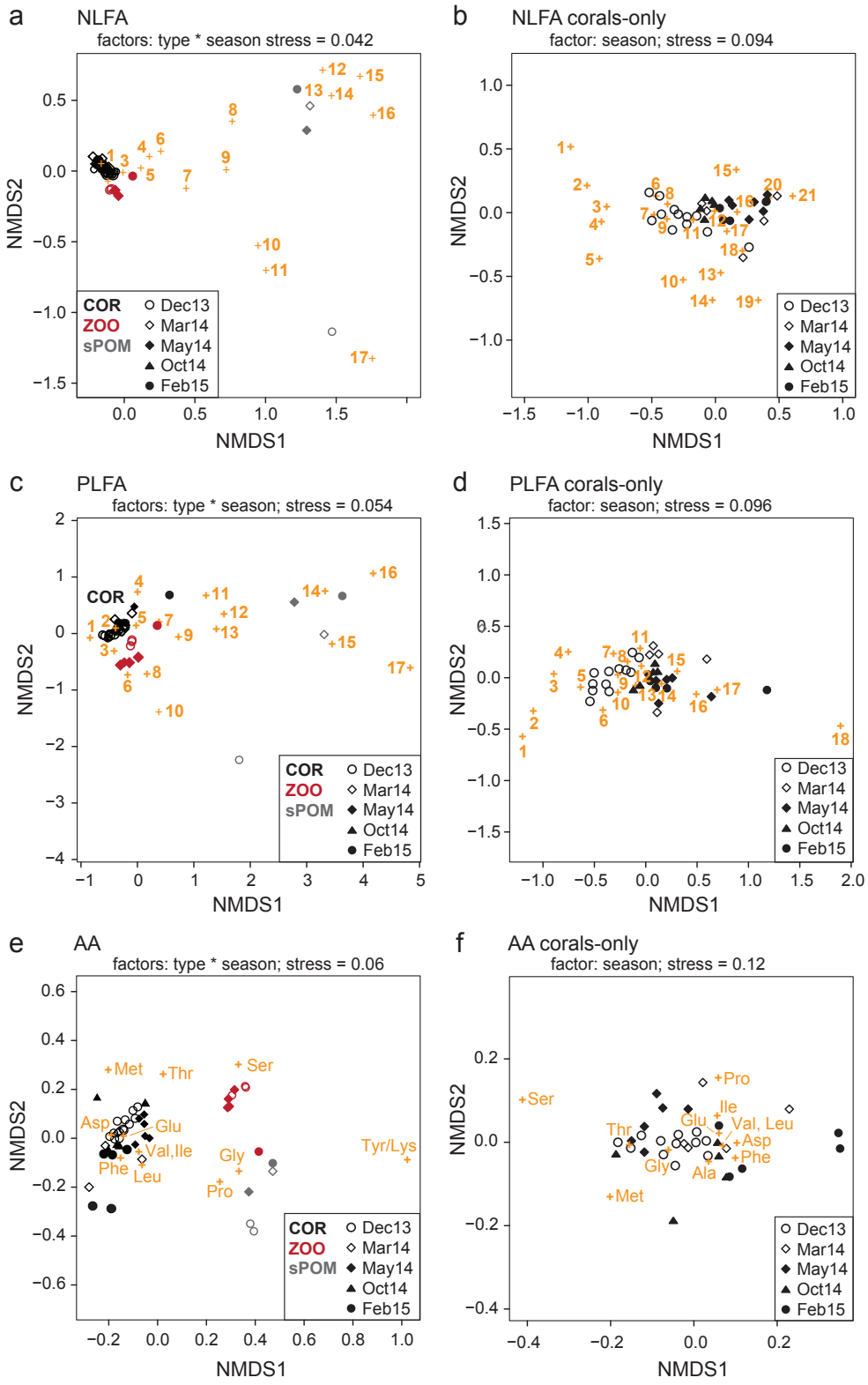

Figure 6: Non-parametric multidimensional scaling (nmds) biplots, illustrating the compositional similarity in neutral-lipid-derived fatty acids (NLFAs), phospholipid-derived fatty acids (PLFAs), and amino acids (AAs), of (a, c, e): corals (black), zooplankton (red) and suspended particulate organic matter (sPOM, grey) between the respective seasons (symbols, see legend); and (b, d, f): of corals-only, between the different seasons. (a, c, e) is analogous to Permanova 1 (factors type x season; Online Resource S2-3), (b, d, f) to Permanova_2 (factor season). Orange numbers indicate compounds, provided as Online Resource S2-2 and in text. Further given is the stress of the nmds.

390 ‘9’, Figure 6c compounds ‘6’). Seasonal differences in coral AA composition were less
391 pronounced (Figure 6f).

392 The coral NLFAs and PLFAs contained zooplankton-, phytoplankton- and bacteria-FATMs
393 (Figure 7). The zooplankton NLFAs and PLFAs likewise comprised zooplankton-,
394 phytoplankton- and bacteria-FATMs, while the sPOM FAs mostly displayed bacteria-

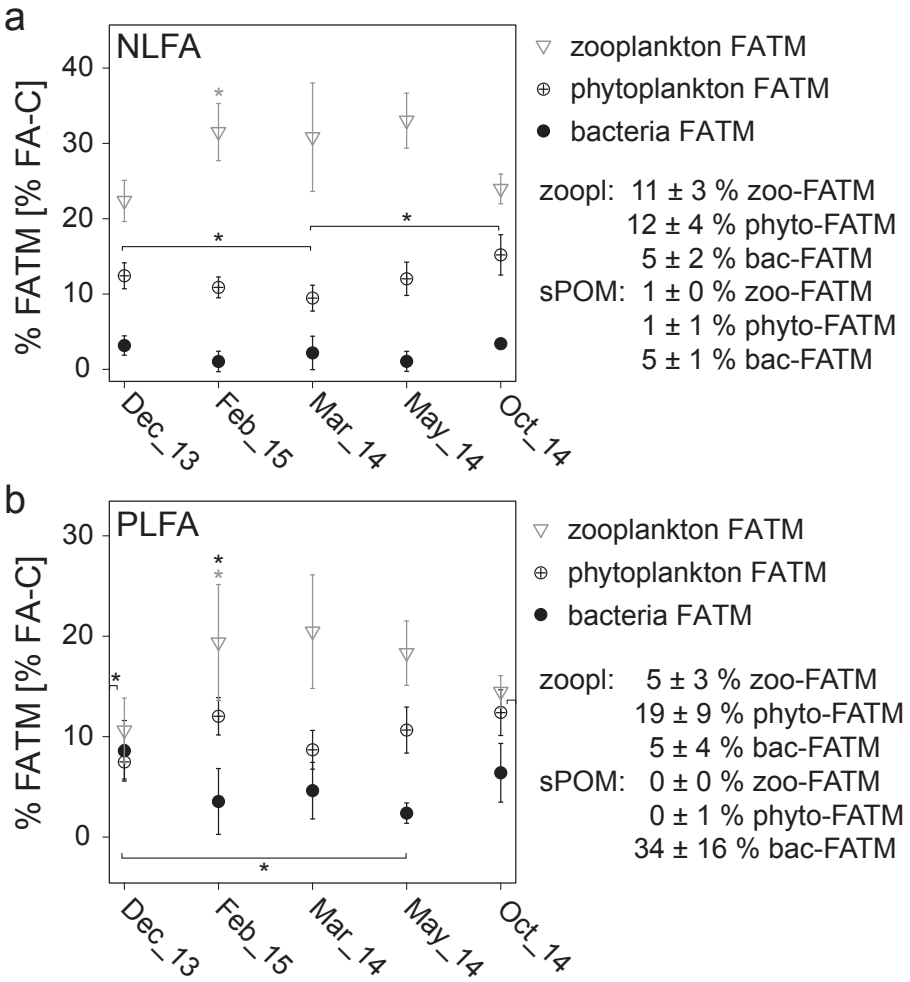

395

396 Figure 7: *Lophelia pertusa* fatty acid trophic markers (FATMs, in % of total fatty-acid-carbon) for
397 zooplankton, phytoplankton and bacteria over the seasons; (a) in neutral-lipid-derived fatty acids
398 (NLFAs); (b) in phospholipid-derived fatty acids (PLFAs). For clearer illustration of seasonal
399 development, the time axis is non-continuous. *: data point(s) significantly different ($p < 0.05$) from
400 previous data point(s)/data point(s) indicated by bracket. Numbers below legend: respective FATMs
401 in zooplankton (zoopl) and suspended particulate organic matter (sPOM).
402

403 FATMs. The percentage of zooplankton-FATMs in *L. pertusa* was higher in February, March
404 and late May, as compared to December and October. The percentage of phytoplankton-
405 FATMs in the coral NLFAs was highest in October and December, in PLFAs in October and
406 February. In October and December, coral PLFAs showed the highest percentage of bacteria-
407 FATMs.
408

409 # Discussion

410 Annual seasonal cycles of light and temperature have profound effects in sunlit surface
411 waters, but also in deep-sea ecosystems (Billett et al. 1983). The seasonal dynamics of
412 temperature and food availability at Nakken reef control the diet and physiology of CWC *L.*
413 *pertusa*, i.e., its metabolic activity, tissue reserves, skeletal growth and reproduction.
414

415 **Seasonal environmental dynamics**

416 The temperature of the deep-water around Nakken reef undergoes an annual cycle
417 characteristic for Norwegian fjords (Bakke and Sands 1977). Higher temperatures in autumn
418 and winter are caused by the intrusion of deep, warmer water from the Norwegian Sea over
419 the fjord sill (Bakke and Sands 1977). Temperatures decrease in late winter, and remain low
420 throughout summer, due to the pronounced water column stratification, established by the
421 spring freshwater flood (Husa et al. 2014b).
422 The availability of sPOM and zooplankton food at Nakken reef follows a seasonal succession
423 typical for high latitude waters. The increasing sPOM concentration from February to March
424 indicates an export of the early phytoplankton bloom from the ocean surface. Such an early
425 phytoplankton bloom is common in Norwegian fjords, which are protected from the
426 counteracting wind-induced vertical transport of the developing phytoplankton below the
427 critical depth (Braarud 1974; Braarud et al. 1974; Husa et al. 2014a). The sPOM-food pulse

428 at Nakken reef ceases by late May, likely related to the senescence of the spring bloom in the
429 surface waters (Braarud 1974), and the progressing water column stratification (Husa et al.
430 2014b), which attenuates the downward transport of phytodetritus. With reduced sPOM
431 availability, zooplankton becomes the most abundant food source in the water column above
432 Nakken reef. Zooplankton performs diurnal vertical migrations between the ocean surface
433 and deep water masses, and could therefore maintain the supply of CWCs with fresh organic
434 matter under stratified conditions (Jónasdóttir et al. 2015; Van Engeland et al. 2019). Low
435 sPOM and zooplankton concentration in December indicate winter food limitation at Nakken
436 reef.
437
438 **Seasonal controls on coral diet**
439 The seasonal succession of sPOM and zooplankton at Nakken reef is reflected in the diet of
440 *L. pertusa*. The combination of different trophic markers suggests a mixed, mostly surface-
441 derived diet, with seasonally varying contributions of phytodetritus, zooplankton and a lower
442 proportion of bacteria/more degraded material. The year-round high percentage of
443 zooplankton FATMs, the lower percentage of phytoplankton FATMs, and the bulk tissue-
444 $\delta^{15}N$-derived trophic level indicate that corals feed mostly on zooplankton, with a smaller
445 share of phytoplankton/-detritus. By contrast, trophic level estimates based on various AA
446 pairs average around two, indicating a phytodetritus-dominated diet. *Lophelia pertusa* is,
447 however, capable of complex N (re-)cycling, utilization of alternative N resources including
448 ammonium and dissolved amino acids, and de novo synthesis of several putatively 'essential'
449 amino acids (Mueller et al 2014; Middelburg et al. 2015). This high metabolic flexibility may
450 complicate the use of AA-$\delta^{15}N$ as trophic marker. For the present study, we consider the
451 trophic level estimates from the bulk tissue $\delta^{15}N$ to be more robust because firstly, the bulk
452 tissue method has been tested on this CWC species in several studies (Duineveld et al. 2004;

453 Kiriakoulakis et al. 2005; van Oevelen et al. 2018), and secondly, the results agree with the
454 FATM-results of the present study. For the AA-method, we suggest controlled feeding
455 experiments (Chikaraichi et al. 2009) to investigate its applicability for *L. pertusa*.
456 Classic analysis (tissue-$\delta^{15}N$, FATM) suggests a diet of phytoplankton and/or zooplankton at
457 varying proportions for *L. pertusa* from the North Atlantic (Kiriakoulakis et al. 2005; van
458 Oevelen et al. 2018), the Bay of Biscay (Duineveld et al. 2004), and the Mediterranean
459 (Carlier et al. 2009). The trophic contribution of zooplankton, phytodetritus, and other
460 resources, such as more degraded sPOM or bacteria varies locally, for instance with reef
461 depth (van Oevelen et al. 2018), but also on a seasonal scale, as we show here. The spring
462 sPOM and zooplankton food pulse at Nakken reef is reflected in an increased coral-$\delta^{13}C$,
463 which indicates feeding on fresher material with a high chlorophyll-a- and correlated $\delta^{13}C$
464 content (Miller et al. 2008), or feeding on a higher trophic level (Fry 2006), such as
465 zooplankton. An increased trophic contribution of zooplankton to the coral diet in spring is
466 corroborated by the increased percentage of zooplankton FATMs, and the peak in tissue-
467 $\delta^{15}N$-derived and AA-$\delta^{15}N$-derived trophic level. The lower $\delta^{13}C$, higher C:N ratio and
468 increased bacteria FATMs in October and December imply a more degraded diet of a lower
469 trophic level during the autumn and winter food limitation.
470
471 **Seasonal controls on coral physiology**
472 The ecological fitness of an organism depends on a close interplay of different physiological
473 functions, including growth in size, storage of tissue reserves, and metabolic activity
474 (Ricklefs and Wikelski 2002). *Lophelia pertusa* at Nakken reef maintains metabolic activity
475 and linear skeletal growth throughout the year, albeit at seasonally variable rates, while
476 showing a build-up and decline of tissue reserves. Oxygen consumption was largely in the
477 range of previous studies (0.07 to 0.30 μmol O_2 $(gDM)^{-1}$ h^{-1}, Maier et al. 2019 and references

478 therein), besides higher rates in October. Linear growth was likewise in the range of previous
479 studies (Brooke and Young 2009 and references therein). Young polyps contribute most to
480 the linear extension of the colony (present study; Mortensen 2001), owing to their high
481 calcification (Maier et al. 2009). The maintenance of linear growth, even under food-
482 limitation, underlines its importance for sessile cold-water corals to escape less-favourable
483 conditions, e.g., enhanced local sedimentation or locally reduced currents and food
484 availability (Brooke and Young 2009).
485 The annual variation in tissue reserves, linear growth, and metabolic activity reflects the
486 seasonal dynamics of the reef environment. From February to late May, *L. pertusa* almost
487 doubles its OC content, underlining its reliance on the spring-bloom related food pulse, and
488 its efficient exploitation and storage (Maier et al. 2019). The acquired resources are initially
489 largely invested in the AA pool, while a pool of NLFAs is built-up later, from October to
490 December. Tissue reorganization and FA build-up in autumn could indicate energy storage
491 for food-limited winter months, as suggested by Dodds et al. (2009), and/or relate to the high
492 oocyte growth during this time of the year (Brooke and Järnegren 2013). The simultaneous
493 increase in metabolic activity in October indicates an enhanced energetic demand, which
494 could result from the tissue modifications. At the same time, increasing temperatures at
495 Nakken reef in autumn partly explained the increase in respiration, endorsing the previously
496 observed low acclimatization capacity to increased temperatures in *L. pertusa* (Dodds et al.
497 2007). During the presumably limited phyto-and zooplankton availability in this season, the
498 consumption of degraded, resuspended sPOM and/or bacteria could facilitate the increased
499 energy investment. Nevertheless, the concurrent reduction of linear growth from October to
500 December (present study), or June to September (Mortensen 2001), could indicate an
501 energetic shortcut, with a trade-off between tissue growth (somatic and reproductive) and

502 calcification, as suggested for tropical corals (Harrison and Wallace 1990; Anthony et al.
503 2002).
504 The >50% drop in OC, FAs and AAs between December and February coincides with the
505 annual spawning season of Norwegian *L. pertusa* (late January to early March; Brooke and
506 Järnegren 2013; Larsson et al. 2013), and indicates the massive release of gametes. A
507 comparable seasonal development of tissue reserves, with a build-up of OC and lipids, and a
508 sudden drop during spawning, has been observed in shallow-water Scleractinians (Oku et al.
509 2003) and gorgonians (Gori et al. 2012; Viladrich et al. 2016). Dodds et al. (2009) reported
510 no statistically significant seasonal pattern of FA concentrations in North Atlantic *L. pertusa*,
511 but their data show a similar trend as the present, with a drop of triacyl-glyceride-derived FA
512 concentration from November to February. The >50% reduction in tissue biomass during the
513 spawning season suggests that reproduction is associated with high costs and energy
514 investments, which is typical for a broad-cast spawning species such as *L. pertusa* (Brooke
515 and Järnegren 2013; Larsson et al. 2014). The spawning season coincides with the period of
516 polyp budding and highest linear growth. The biomass-depleted, fast-growing corals likely
517 profit from the exploitation of the simultaneously starting spring bloom, underlining the
518 seasonal environmental forcing on CWC life history.
519
520 **An annual cycle of a cold-water coral**
521 The present study demonstrates that tissue biomass and composition, metabolic activity and
522 linear growth of *L. pertusa* undergo a pronounced seasonal cycle, driven by the interplay of
523 seasonally-variable temperature and food availability (Figure 8). In spring, *L. pertusa* builds
524 up OC and AA reserves, profiting from the enhanced phyto- and zooplankton production of
525 the spring bloom. During autumn, the corals reorganize their tissue reserves, accompanied by
526 an increase in metabolic activity, which may be linked to the rapid gametogenesis at this time

of the year (Brooke and Järnegren 2013). The related energetic investment could be facilitated by the consumption of more degraded, resuspended sPOM and/or bacteria, since phyto-and zooplankton is presumably limited. However, the simultaneous reduction in linear skeletal growth reveals a potential energetic shortage. A sudden, >50%- drop of tissue biomass between December and February indicates the annual spawning activity of the corals, perfectly timed for the larvae and biomass-depleted adults to exploit the upcoming spring phytoplankton bloom, increase tissue stocks, catch-up with linear growth, bud polyps and hereby restart the annual cycle.

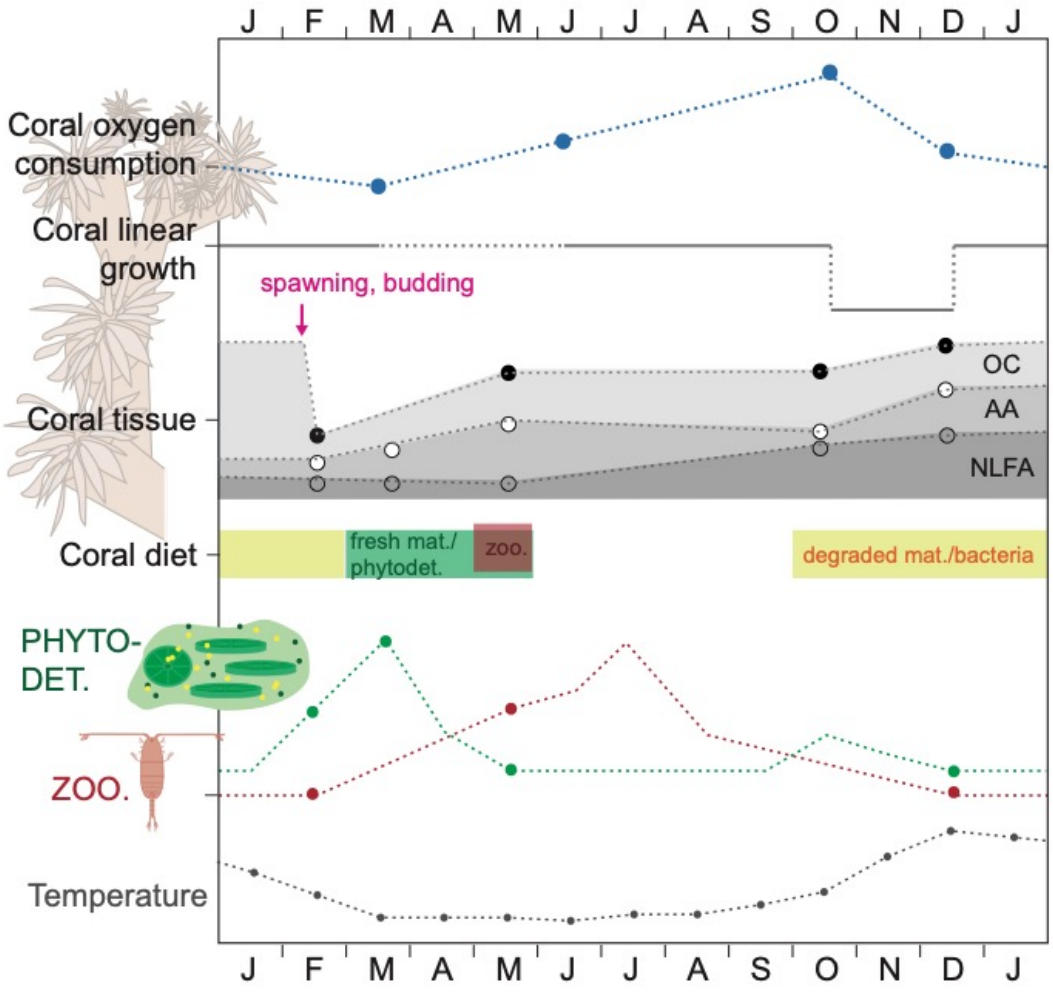

Figure 8: Annual cycle of a cold-water coral: Dots/solid lines: measurements; dotted lines: extrapolations, for phytodetritus according to Braarud et al. (1974), with the exception that no export of phytoplankton as phytodetritus is assumed in summer due to stratification (Husa et al. 2014b). Extrapolation for zooplankton according to Gundersen (1953), Lie (1967). 'Zoo'.: zooplankton; 'phytodet'.: phytodetritus; 'fresh/degraded mat.': fresh/degraded material; 'NLFA': neutral-lipid-derived fatty acids; 'AA': amino acids; 'OC': organic carbon.

Global change acts upon the seasonal environmental variability, which controls the phenology of organisms, i.e., their seasonal timing of activities (Walther et al. 2002). Our study shows that deep-sea species like *L. pertusa* display a pronounced phenology, and may therefore be highly sensitive towards changes in the seasonal forcing. Increased temperatures and ocean acidification may increase their metabolic and growth costs (Dodds et al. 2007; McCulloch et al. 2012), while enhanced stratification could decrease export production and food availability (Bopp et al. 2001; Soetaert et al. 2016). Exacerbating already existing seasonal energetic constraints will impact their growth and reproduction capacities, with potentially severe consequences for the health and distribution of the deep-sea CWC ecosystems.

Conflict of interest

On behalf of all authors, the corresponding author states that there is no conflict of interest.

References

Addamo AM, Vertino A, Stolarski J, García-Jiménez R, Taviani M, Machordom A (2016) Merging scleractinian genera: the overwhelming genetic similarity between solitary *Desmophyllum* and colonial *Lophelia*. BMC Evolutionary Biology 16:108

Albretsen J (2011) NorKyst-800 report no. 1: User manual and technical descriptions. Fisken og havet

Anthony KRN, Connolly SR, Willis BL (2002) Comparative analysis of energy allocation to tissue and skeletal growth in corals. Limnology and Oceanography 47:1417–1429

Bakke JLW, Sands NJ (1977) Hydrographical studies of Korsfjorden, western Norway, in the period 1972–1977. Sarsia 63:7–16

Billett DSM, Lampitt RS, Rice AL, Mantoura RFC (1983) Seasonal sedimentation of phytoplankton to the deep-sea benthos. Nature 302:520

Blaud A, Lerch TZ, Chevallier T, Nunan N, Chenu C, Brauman A (2012) Dynamics of bacterial communities in relation to soil aggregate formation during the decomposition of ^{13}C-labelled rice straw. Applied Soil Ecology 53:1–9

Bopp L, Monfray P, Aumont O, Dufresne J-L, Le Treut H, Madec G, Terray L, Orr JC (2001) Potential impact of climate change on marine export production. Global Biogeochemical Cycles 15:81–89

Boschker HTS, de Brouwer JFC, Cappenberg TE (1999) The contribution of macrophyte-derived organic matter to microbial biomass in salt-marsh sediments: Stable carbon isotope analysis of microbial biomarkers. Limnology and Oceanography 44:309–319

Braarud T (1974) The natural history of the Hardangerfjord. Sarsia 55:99–114

Braarud T, Föyn Hofsvang B, Hjelmfoss P, Överlanda Aa-K (1974) The natural history of the Hardangerfjord 10. The phytoplankton in 1955–56. The quantitative phytoplankton cycle in the fjord waters and in the offshore coastal waters. Sarsia 55:63–98

Brooke S, Järnegren J (2013) Reproductive periodicity of the scleractinian coral *Lophelia pertusa* from the Trondheim Fjord, Norway. Mar Biol 160:139–153

Brooke S, Young CM (2009) In situ measurement of survival and growth of *Lophelia pertusa* in the northern Gulf of Mexico. Marine Ecology Progress Series 397:153–161

Carlier A, Le Guilloux E, Olu K, Sarrazin J, Mastrototaro F, Taviani M, Clavier J (2009) Trophic relationships in a deep Mediterranean cold-water coral bank (Santa Maria di Leuca, Ionian Sea). Marine Ecology Progress Series 397:125–137

Chikaraishi Y, Ogawa NO, Kashiyama Y, Takano Y, Suga H, Tomitani A, Miyashita H, Kitazato H, Ohkouchi N (2009) Determination of aquatic food-web structure based on compound-specific nitrogen isotopic composition of amino acids. Limnology and Oceanography: Methods 7:740–750

593 Dalsgaard J, St. John M, Kattner G, Müller-Navarra D, Hagen W (2003) Fatty acid trophic
594 markers in the pelagic marine environment. In: Southward A.J., Tyler P.A., Young
595 C.M., Fuiman L.A. (eds) Advances in marine biology. Elsevier Science Ltd., pp 225–
596 340

597 Dodds LA, Black KD, Orr H, Roberts JM (2009) Lipid biomarkers reveal geographical
598 differences in food supply to the cold-water coral *Lophelia pertusa* (Scleractinia).
599 Marine Ecology Progress Series 397:113–124

600 Dodds LA, Roberts JM, Taylor AC, Marubini F (2007) Metabolic tolerance of the cold-water
601 coral *Lophelia pertusa* (Scleractinia) to temperature and dissolved oxygen change.
602 Journal of Experimental Marine Biology and Ecology 349:205–214

603 Duineveld GCA, Lavaleye MSS, Berghuis EM (2004) Particle flux and food supply to a
604 seamount cold-water coral community (Galicia Bank, NW Spain). Marine Ecology
605 Progress Series 277:13–23

606 Duineveld GCA, Lavaleye MSS, Bergman MJN, De Stigter H, Mienis F (2007) Trophic
607 structure of a cold-water coral mound community (Rockall Bank, NE Atlantic) in
608 relation to the near-bottom particle supply and current regime. Bulletin of Marine
609 Science 81:449–467

610 Falk-Petersen S, Dahl TM, Scott CL, Sargent JR, Gulliksen B, Kwasniewski S, Hop H,
611 Millar R-M (2002) Lipid biomarkers and trophic linkages between ctenophores and
612 copepods in Svalbard waters. Marine Ecology Progress Series 227:187–194

613 Frederiksen R, Jensen A, Westerberg H (1992) The distribution of the scleractinian coral
614 *Lophelia pertusa* around the Faroe islands and the relation to internal tidal mixing.
615 Sarsia 77:157–171

616 Freiwald A (2002) Reef-forming cold-water corals. In: Wefer G., Billett D., Hebbeln D.,
617 Joergensen B.B., Schlueter M., van Weering T.C.E. (eds) Ocean Margin Systems.
618 Springer-Verlag Berlin Heidelberg, pp 365–385

619 Fry B (2006) Stable Isotope Ecology. Springer, New York, US

620 Gori A, Viladrich N, Gili J-M, Kotta M, Cucio C, Magni L, Bramanti L, Rossi S (2012)
621 Reproductive cycle and trophic ecology in deep versus shallow populations of the
622 Mediterranean gorgonian Eunicella singularis (Cap de Creus, northwestern
623 Mediterranean Sea). Coral Reefs 31:823–837

624 Grosse J, van Breugel P, Boschker HTS (2015) Tracing carbon fixation in phytoplankton-
625 compound specific and total ^{13}C incorporation rates. Limnology and Oceanography:
626 Methods 13:288–302

627 Gundersen KR (1953) Zooplankton investigations in some fjords in Western Norway during
628 1950-1951.

629 Harrison PL, Wallace CC (1990) Reproduction, dispersal and recruitment of scleractinian
630 corals. Ecosystems of the world. pp 1–373

631 Howell KL, Pond DW, Billett DSM, Tyler PA (2003) Feeding ecology of deep-sea seastars
632 (Echinodermata: Asteroidea): a fatty-acid biomarker approach. Marine Ecology
633 Progress Series 255:193–206

634 Husa V, Kutti T, Ervik A, Sjøtun K, Hansen PK, Aure J (2014a) Regional impact from fin-
635 fish farming in an intensive production area (Hardangerfjord, Norway). Marine
636 Biology Research 10:241–252

637 Husa V, Steen H, Sjøtun K (2014b) Historical changes in macroalgal communities in
638 Hardangerfjord (Norway). Marine Biology Research 10:226–240

639 Jónasdóttir SH, Visser AW, Richardson K, Heath MR (2015) Seasonal copepod lipid pump
640 promotes carbon sequestration in the deep North Atlantic. PNAS 112:12122–12126

641 Kelly JR, Scheibling RE (2012) Fatty acids as dietary tracers in benthic food webs. Marine
642 Ecology Progress Series 446:1–22

643 Kiriakoulakis K, Fisher E, Wolff G, Freiwald A, Grehan A, Roberts J (2005) Lipids and
644 nitrogen isotopes of two deep-water corals from the North-East Atlantic: initial results
645 and implications for their nutrition. In: Freiwald A., Roberts J. (eds) Cold-water
646 corals and ecosystems. Springer, Berlin, Heidelberg, pp 715–729

647 Larsson AI, Järnegren J, Strömberg SM, Dahl MP, Lundälv T, Brooke S (2014)
648 Embryogenesis and larval biology of the cold-water coral *Lophelia pertusa*. PLOS
649 ONE 9:e102222

650 Larsson AI, Lundälv T, van Oevelen D (2013) Skeletal growth, respiration rate and fatty acid
651 composition in the cold-water coral *Lophelia pertusa* under varying food conditions.
652 Marine Ecology Progress Series 483:169–184

653 Lartaud F, Meistertzheim AL, Peru E, Le Bris N (2017) *In situ* growth experiments of reef-
654 building cold-water corals: the good, the bad and the ugly. Deep Sea Research Part I:
655 Oceanographic Research Papers 121:70–78

656 Lavaleye M, Duineveld G, Lundälv T, White M, Guihen D, Kiriakoulakis K, Wolff GA
657 (2009) Cold-water corals on the Tisler reef: preliminary observations on the dynamic
658 reef environment. Oceanography 22:76–84

659 Lie U (1967) The natural history of the Hardangerfjord 8. Quantity and composition of the
660 zooplankton, September 1955 – September 1956. Sarsia 30:49–74

661 Maier C, Hegeman J, Weinbauer MG, Gattuso J-P (2009) Calcification of the cold-water
662 coral *Lophelia pertusa* under ambient and reduced pH. Biogeosciences 6:1875–1901

663 Maier SR, Kutti T, Bannister RJ, Breugel P van, Rijswijk P van, Oevelen D van (2019)
664 Survival under conditions of variable food availability: resource utilization and
665 storage in the cold-water coral *Lophelia pertusa*. Limnology and Oceanography
666 9999:1–21

667 Martinez Arbizu, P. (2019). pairwiseAdonis: Pairwise multilevel comparison using adonis. R
668 package version 0.3

669 McClelland JW, Montoya JP (2002) Trophic relationships and the nitrogen isotopic
670 composition of amino acids in plankton. Ecology 83:2173–2180

671 McCulloch M, Falter J, Trotter J, Montagna P (2012) Coral resilience to ocean acidification
672 and global warming through pH up-regulation. Nature Climate Change 2:623–627

673 Michener R, Lajtha K (2008) Stable isotopes in ecology and environmental science.
674 Blackwell Publishing Ltd

675 Middelburg JJ, Mueller CE, Veuger B, Larsson AI, Form A, van Oevelen D (2015)
676 Discovery of symbiotic nitrogen fixation and chemoautotrophy in cold-water corals.
677 Scientific Reports 5:17962:1–9

678 Miller TW, Brodeur RD, Rau GH (2008) Carbon stable isotopes reveal relative contribution
679 of shelf-slope production to the Northern California Current pelagic community.
680 Limnology and Oceanography 53:1493–1503

681 Mortensen PB (2001) Aquarium observations on the deep-water coral *Lophelia pertusa* (L.,
682 1758) (scleractinia) and selected associated invertebrates. Ophelia 54:83–104

683 Mueller CE, Larsson AI, Veuger B, Middelburg JJ, Van Oevelen D (2014) Opportunistic
684 feeding on various organic food sources by the cold-water coral *Lophelia pertusa*.
685 Biogeosciences 11:123–133

686 van Oevelen D, Duineveld GCA, Lavaleye MSS, Kutti T, Soetaert K (2018) Trophic
687 structure of cold-water coral communities revealed from the analysis of tissue
688 isotopes and fatty acid composition. Marine Biology Research 14:287–306

689 Ogle DH, Wheeler P, Dinno A (2018) FSA: Fisheries Stock Analysis. R package version
690 0.8.22, https://github.com/droglenc/FSA.

691 Oksanen J, Blanchet GF, Friendly M, Kindt R, Legendre P, McGlinn D, Minchin PR, O'Hara
692 RB, Simpson GL, Solymos P, Stevens MHH, Szoecs E, Wagner H (2018) vegan:
693 Community Ecology Package, https://CRAN.R-project.org/package=vegan.

694 Oku H, Yamashiro H, Onaga K, Sakai K, Iwasaki H (2003) Seasonal changes in the content
695 and composition of lipids in the coral *Goniastrea aspera*. Coral Reefs 22:83–85

696 Post DM, Layman CA, Arrington DA, Takimoto G, Quattrochi J, Montaña CG (2007)
697 Getting to the fat of the matter: models, methods and assumptions for dealing with
698 lipids in stable isotope analyses. Oecologia 152:179–189

699 R Core Team (2017) R: A language and environment for statistical computing. R Foundation
700 for Statistical Computing, Vienna, Austria. URL https://www.R-project.org/.

701 Ricklefs RE, Wikelski M (2002) The physiology/life-history nexus. Trends in Ecology &
702 Evolution 17:462–468

703 Roberts JM, Wheeler AJ, Freiwald A (2006) Reefs of the deep: the biology and geology of
704 cold-water coral ecosystems. Science 312:543–547

Smyntek PM, Teece MA, Schulz KL, Thackeray SJ (2007) A standard protocol for stable isotope analysis of zooplankton in aquatic food web research using mass balance correction models. Limnology and Oceanography 52:2135–2146

Soetaert K, Mohn C, Rengstorf A, Grehan A, van Oevelen D (2016) Ecosystem engineering creates a direct nutritional link between 600-m deep cold-water coral mounds and surface productivity. Scientific Reports 6:35057:

Thiem Ø, Ravagnan E, Fosså JH, Berntsen J (2006) Food supply mechanisms for cold-water corals along a continental shelf edge. Journal of Marine Systems 60:207–219

Van Engeland T, Godø OR, Johnsen E, Duineveld GCA, van Oevelen D (2019) Cabled ocean observatory data reveal food supply mechanisms to a cold-water coral reef. Progress in Oceanography 172:51–64

Veuger B, Middelburg JJ, Boschker HTS, Houtekamer M (2005) Analysis of ^{15}N incorporation into D-alanine: a new method for tracing nitrogen uptake by bacteria. Limnology and Oceanography: Methods 3:230–240

Viladrich N, Bramanti L, Tsounis G, Chocarro B, Martínez-Quitana A, Ambroso S, Madurell T, Rossi S (2016) Variation in lipid and free fatty acid content during spawning in two temperate octocorals with different reproductive strategies: surface versus internal brooder. Coral Reefs 35:1033–1045

Walther G-R, Post E, Convey P, Menzel A, Parmesan C, Beebee TJC, Fromentin J-M, Hoegh-Guldberg O, Bairlein F (2002) Ecological responses to recent climate change. Nature 416:389

Acknowledgements

We are grateful to the crew of the RV *H. Mosby* and RV *G.O. Sars*, and the pilots of the ROV *Aglantha*. We would like to thank Peter van Breugel and Pieter van Rijswijk (NIOZ) for their help in chemical analysis. Funding was provided by the Royal Netherlands Academy of Arts and Sciences (KNAW) Fund (KNAWWF/807/19022 to SRM), the Netherlands Organisation for Scientific Research (VIDI grant 864.13.007 to DvO) and the Norwegian Research Council (RCN project no. 244604/E40 to TK).

Data availability

All raw data are available at http://doi.org/10.5281/zenodo.3566881.

Figure legends

Figure 1: Study site and transplantation experiment. (a) Location of Nakken reef at the intersection of Hardanger and Langenuen fjord, western Norway. (b) Live coral colonies (*Lophelia pertusa*) grow in patches on a base of dead coral framework, particularly densely in an area of elevated seafloor (c, indicated by arrow). (d) Workflow of transplantation experiment (OC: organic carbon, ON: organic nitrogen, FA: fatty acids, AA: amino acids, SI: stable isotopes).

Figure 2: Seasonality of the environment at Nakken reef: Modelled temperature (in black) 6 m above bottom, and food availability, i.e., concentration of suspended particulate organic carbon (sPOC, in green) 3-5 m above the reef, and zooplankton-C-concentration (in red) in the water column above the reef. Letters: months from October 2013 to February 2015.

Figure 3: Seasonal environmental controls on tissue reserves and metabolic activity of *Lophelia pertusa*. (a, b) seasonal control of food availability (concentration of suspended particulate organic carbon, i.e., sPOC, and zooplankton; in grey) on coral organic carbon (OC) content (in black); (c) tissue pools amino acids (AA), neutral-and phospholipid-derived fatty acids (NLFA, PLFA) in relation to total coral OC; (d) oxygen consumption (in black) in relation to modelled temperature (in grey). All coral parameters are normalized to coral dry mass (DM). For clearer illustration of seasonal development, the time axis is non-continuous. *: data point(s) significantly different ($p < 0.05$) from previous data point(s)/data point indicated by bracket.

Figure 4: (a) Linear extension of *Lophelia pertusa* old, young, and newly formed terminal polyps over the indicated time periods. Numbers above bars indicate the numbers of

examined polyps. *: linear extension (mean of old, young, new) in this period significantly different from previous period. (b) Old, young and new terminal polyps.

Figure 5: Isotope $\delta^{13}C$ and $\delta^{15}N$ composition of *Lophelia pertusa,* zooplankton and suspended particulate organic matter (sPOM). (a) $\delta^{13}C\delta^{15}N$ composition of corals (black) in comparison with zooplankton (red) and sPOM (grey) over the seasons (legend). (b) like (a), but with fatty-acid corrected $\delta^{13}C$ values. (c) $\delta^{15}N$ of coral tissue and the amino acids glutamic acid/glutamine and phenylalanine over the seasons; in red: trophic level calculated from $\delta^{15}N_{Glu}$ and $\delta^{15}N_{Phe}$ based on Chikaraichi et al., 2009. *: data point significantly different ($p < 0.05$) from previous data point.

Figure 6: Non-parametric multidimensional scaling (nmds) biplots, illustrating the compositional similarity in neutral-lipid-derived fatty acids (NLFAs), phospholipid-derived fatty acids (PLFAs), and amino acids (AAs), of (a, c, e): corals (black), zooplankton (red) and suspended particulate organic matter (sPOM, grey) between the respective seasons (symbols, see legend); and (b, d, f): of corals-only, between the different seasons. (a, c, e) is analogous to Permanova 1 (factors type x season; Online Resource S2-3), (b, d, f) to Permanova_2 (factor season). Orange numbers indicate compounds, provided as Online Resource S2-2 and in text. Further given is the stress of the nmds.

Figure 7: *Lophelia pertusa* fatty acid trophic markers (FATMs, in % of total fatty-acid-carbon) for zooplankton, phytoplankton and bacteria over the seasons; (a) in neutral-lipid-derived fatty acids (NLFAs); (b) in phospholipid-derived fatty acids (PLFAs). For clearer illustration of seasonal development, the time axis is non-continuous. *: data point(s) significantly different ($p < 0.05$) from previous data point(s)/data point(s) indicated by

bracket. Numbers below legend: respective FATMs in zooplankton (zoopl) and suspended particulate organic matter (sPOM).

Figure 8: Annual cycle of a cold-water coral: Dots/solid lines: measurements; dotted lines: extrapolations, for phytodetritus according to Braarud et al. (1974), with the exception that no export of phytoplankton as phytodetritus is assumed in summer due to stratification (Husa et al. 2014b). Extrapolation for zooplankton according to Gundersen (1953), Lie (1967). 'Zoo'.: zooplankton; 'phytodet'.: phytodetritus; 'fresh/degraded mat.': fresh/degraded material; 'NLFA': neutral-lipid-derived fatty acids; 'AA': amino acids; 'OC': organic carbon.